On the homogeneity of a thick layer of mixed granules in optical quality inspection

Bakker, Maarten; Xia, Han

Publication date
2016

Document Version
Final published version

Published in
Proceedings SUM2016, 3rd Symposium on Urban Mining and Circular Economy

Citation (APA)
Bakker, M., & Xia, H. (2016). On the homogeneity of a thick layer of mixed granules in optical quality inspection. In *Proceedings SUM2016, 3rd Symposium on Urban Mining and Circular Economy* (pp. 1-10). CISA Publisher.

ON THE HOMOGENEITY OF A THICK LAYER OF MIXED GRANULES IN OPTICAL QUALITY INSPECTION

M.C.M. Bakker, Han Xia

Resources and Recycling group, Department of Civil Engineering and Geosciences, Delft University of Technology, Stevinweg1, 2628CN, The Netherlands

ABSTRACT: Optical inspection of a thick layer of granules for foreign particles does not directly reveal their true number and the more so if the layer is not homogenous. This raises questions such as “how do I know if the layer is homogenous?” and “what is the relation between the observable particles and the true number?” In this work a theory is proposed for granules with a minority of flat plates that explains their statistical properties under the homogenous condition. Moreover, it offers a simple test for homogeneity or, vice-versa, a way to calculate the true contents in a thick homogenous layer from surface observations of the number of plates. The theory is tested successfully on a uniform ball batch and on dry and moist 2-8 mm gravel batches. The latter served as scaled lab-simulations of a concrete demolition waste stream.

KEYWORDS: granular materials; particle segregation; material packing; homogenous statistics; quality inspection;

1. INTRODUCTION

Surface scanning sensor techniques such as visual cameras, NIR and HSI [Bonifazi, 2015] are in growing demand in the recycling industry due to their excellent performance to price ratio. But also an emerging stand-off laser technique such as LIBS [Xia, 2014] is finding its way to an industry that is hungry for quantitative information and more efficient ways of obtaining it. A common method to employ these techniques for quality inspection is to sample the waste stream, or divert a small sample stream, and present the sample in a monolayer to the sensor. The sensor data are accumulated to build statistics, resulting in an average per sampled unit of volume. For LIBS a similar approach can be applied, except that all the particles in the sample should be presented in single file formation. Point is that all such special measures intervene with the primary recycling process and increase costs. It would be far preferable if the sensor could be positioned directly above an existing conveyor belt which transports the material in bulk as part of the primary process. Unfortunately, this is as yet not an option because there is no theory to predict the relation between sensor readings and the material contents in the granular bulk, even if there is homogeneity. Moreover, there is also no theory

Proceedings SUM2016, Third Symposium on Urban Mining and Circular Economy, 23 - 25 May 2016
Old Monastery of St. Augustine, Bergamo, Italy

available to predict how a homogenous layer of granules would present foreign particles to the sensor, i.e., how many would appear at its free surface. This work proposes a theory to resolve these issues for uniform sized granules and a minority of uniform plates. But this is just a first step in improving our understanding of how a homogenous granular material may accommodate a minority of foreign particles. As a next step this theory is extended to a size range of granules and more complex shaped foreign particles. The assumptions behind this daring extension are that, as a minority, the foreign particles do not interact, while their incidental presence forms a small localized disturbance to the granule packing. In that sense, a degree of variation in foreign particle shape should change very little. On the other hand, the granule packing and its capacity to store foreign particles will surely be affected by size differences. But then again, if it concerns a moderate size variation that is the same for granules and foreign particles, it is expected that the relative influences cancel with respect to the average sized particle. This gives rise to the notion of a uniform particle being representative for a much more complex granular mixture. The relevance of this case is that it is representative for a scaled lab version of a concrete demolition waste stream, which materials can be recycled as aggregates into new concrete depending on their quality [Xia, 2013; López-Gayarre, 2009]. Homogeneity is disturbed by particle segregation mechanisms that are activated by vibrations and made worse by gravity. Even the act of mixing, intended to render the material homogenous, may fail due to the nature of the particles in relation to the mixing method used [Ottino, 2000]. Worse yet, different mechanisms may be active at the same time which makes their identification even more complicated. For these reasons much research is devoted to gaining a better understanding and predictability of segregation [Schröter, 2006]. Nevertheless, based on the knowledge of how and how much the material state deviates from the homogenous condition, it may be possible to infer which segregation mechanism is at work and where it originates from in the processing line.

2. Homogeneous statistics

2.1 Building the theory

The act of counting the number of flat plates at the finite free surface of a granular material may be regarded as a sampling problem with the N surface particles as the sample size. The sampling result complies with a binomial distribution with probability p for observing a target particle and 1-p if not, and with expected number E_P and standard deviation STD^B. In the present work the target particles form a number minority of flat plates (1%) by which the exact probability p of finding N^P plates on the surface may be estimated from an analysis of the random sample contents itself as $p \sim N^P/N$:

$$Ep = Np, \quad STD^B = \sqrt{p(1-p)N} \approx \sqrt{N^P} \qquad \text{Eq.(1)}$$

This experimental estimate improves with sample size and does not require a-priori knowledge of the exact numbers of particles in the batch. Thus, even in case a few particles from the batch get lost during testing the estimate will still be accurate. The purpose of mixing a batch is to make it homogenous, and the fact it also changes the precise packing of the materials is commonly not of any consequence in practice. This implies that the resulting precise packing, which is a matter of probability, is not of consequence for what is generally considered to be a satisfactory homogenous mixture. Also, proper mixing does not significantly modify the initial bulk volume. The main conclusion from all this is that any perceivable packing of these same materials that returns the initial material bulk volume is theoretically possible and may be used to predict the homogeneous statistics. The ansatz in the following theory is that any fitting organized packing using the same same-sized particles will predict the correct homogeneous statistics of the material at hand. In this work all the granules are represented by a uniform particle that matches the average shape and size of the granules. It is noted that the sphere is a good approximation for the average shape of all granules used in our experiments.

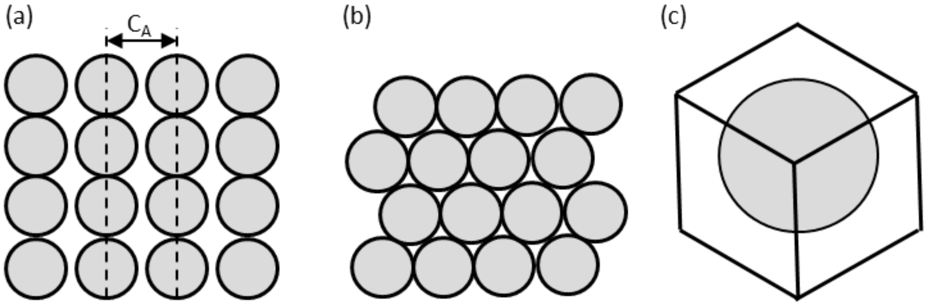

Figure 1: (a) A scalable regular packing of uniform spheres and (b) a fixed regular packing with cannonball stacking in one direction. (c) A cubic positioning cell with square facets tightly envelopes a sphere and provides 6 positions (3 dependent) for a flat plate which average size is approximately equal to the sphere diameter.

Figure 1a and b depict two regular packings that can represent the unknown packing of our two types of experimental material. It is paramount that the number of spheres and packing matches the bulk density in the experiment. To this end, the row spacing in Fig. 1a can be increased by compaction parameter C_A>=1, where C_A=1 complies with highest density. In Fig. 1b the number of spheres in the direction of cannonball stacking can be slightly increased by a small compaction parameter C_B>=1. It is noted that the granular bulk density depends on the surface to volume ratio due to surface packing effects, by which a calibration must apply the same material volume and shape as used in the calculations. For a box-shaped volume of dimensions (L, W, H) the number of spheres occupying the upper layer of the top surface is N^{SS} and the total number spanning the whole volume is N^{SV}.

$$N^{SS} = \frac{LW}{(C_A d)^2}, \quad N^{SV} = N^{SS}\frac{H}{d} \qquad \text{(Fig. 1a)}$$

$$N^{SS} = C_B\left(\frac{L}{d}-\frac{1}{2}\right)\frac{W}{d}, \quad N^{SV} = N^{SS}\frac{H-\delta}{d-\delta} \qquad \text{(Fig. 1b)}$$

Eq.(2)

It is noted we allow for fractional numbers to obtain a better fit in case of small material volumes. Here d is the diameter of the sphere and the geometrical constant is δ = 0.441mm. The positions available in the matrix to a plastic plate are determined by 3D positon-fixed, multifaceted cells which incorporate a sphere. The motivation for using fixed cells and fixed sphere packing is that the plates form a small minority and are (about) the same size as the granules. Therefore, the presence of a plate will at most cause a small local disturbance to the packing, which influence may be neglected. The probability of finding two or more plates next to the same granule is so remote that it may also be neglected. The cell type is selected to envelop the sphere tightly, while the shape and size of its identical facets should match the plate size and shape to close approximation. A plate locked in a typical granular packing has one rotational plane in which its reorientation minimizes the displacement of adjacent granules. The positioning cell may be regarded as a discrete, position fixed implementation of the free-volume theory for granular mixtures [Oversteegen, 2004]. The rotational plane is determined by the way the plate is clamped in between at least two granules, which in the context of the theory complies with the freedom to rotate within a cell facet. For the relatively symmetrical materials used in this work the rotational degree of freedom is uniform throughout the packing and its surface, and therefore does not play a role in the following theory. Figure 1c shows the square cell that closely fits these criteria for our experimental materials.

2.2 Homogenous equations

The number of cells in each direction of the material volume of dimensions (L,W,H) is the same as the number of spheres, but is detailed here for clarity:

$$N^{CL} = \frac{L}{C_A d},\quad N^{CW} = \frac{W}{C_A d},\quad N^{CH} = \frac{H}{d},\qquad \text{(Fig. 1a)}$$

$$N^{CL} = C_B\left(\frac{L}{d} - \frac{1}{2}\right),\quad N^{CW} = \frac{W}{d},\quad N^{CH} = \frac{H-\delta}{d-\delta},\qquad \text{(Fig. 1b)} \qquad \text{Eq.(3)}$$

The number of positions available to a square plate in the closed rectangular volume is determined by the total number of independent facets N^{FV}.

$$N^{FV} = 3\mathrm{N}^{CH}\mathrm{N}^{CW}\mathrm{N}^{CL} + \mathrm{N}^{CH}\mathrm{N}^{CW} + \mathrm{N}^{CH}\mathrm{N}^{CL} + \mathrm{N}^{CW}\mathrm{N}^{CL} \qquad \text{Eq.(4)}$$

The number of positions (N^{PS}) in the upper surface layer in which a square plate could be detected by the human eye as being directly in or on this upper layer is:

$$N^{FS} = 3\mathrm{N}^{CW}\mathrm{N}^{CL} + \mathrm{N}^{CL} + \mathrm{N}^{CW} \qquad \text{Eq.(5)}$$

After matching the packing parameters to the experimental uniform batch, the number of spheres may differ slightly from the number of granules due to small differences in surface packing between the idealizing model and reality. In view of the binomial statistics it is a requirement that the ratio of plates to spheres equals the experimental ratio. We therefore correct the number of plates N^{NP} used in the calculations according to:

$$N^{NP} = \alpha N^{SV} \qquad \text{Eq.(6)}$$

This leads to the expected number E^P in Eq. (1) of the number of plates that is detectable in or on the upper layer of the free top surface of the box volume when the material is homogenous.

$$E^P = Np = N^{NP} N^{FS} / N^{FV} \qquad \text{Eq. (7)}$$

3. Materials and method

3.1 Uniform batch

The uniform batch (cf. Fig. 2a) consists of identical PVC balls (though not perfectly spherical) and identical square polypropylene plates. The parameters are listed in Tab. 1. To test for the influence of possible particle segregation effects we use a dry batch and a batch wetted with a thin type of oil to act as a mild sticking agent. This oil eliminates plate percolation and yet still allows the plates to be easily transferred between balls during mixing.

Table 1: Composition of the uniform batch in the tests. γ is the ratio of batch bulk density and ball mass density. For calibration of packing and bulk density a comparable volume of material was used.

	nr	Size [mm]	Mass [g]	(bulk) density [kg/m^3]	Volume (LxWxH) [mm]
plates	56	9 x 9 x 1	0.072	895	
Balls	5600	10.7(diam.)	0.897	1399	
batch	5656			658 (γ= 0.470)	370 x 260 x 85

The material is mixed in a rectangular wooden box of twice the height of the material volume to minimize surface influences and obtain a proper mixing by tumbling motions the balls. In addition, the inner walls of the box were lined with a plastic fibre mesh to minimize particle friction (dry material) and particle stick-slip (oiled). The mesh effectively decreased the wall surface by 75%, leaving the balls surface to dominate in the experiments. The top lid was opened after each mixing session to count the plates that were detectable in the upper layer of the free material surface. Detection by eye was facilitated by the choice of red plates and blue balls. Two of the blue balls were replaced with identical red ones to serve as a sensitive control statistics for proper mixing. The probability of finding one red ball in the material surface in the box was 0.15 (number of surface balls divided by all balls) with an expected number of 9 for the 2 red balls in a series of 30 experiments. A thorough, but carefully designed mixing procedure was applied to ensure the batch could be mixed to a state of homogeneity. The box was first manually rotated a few times in the directions perpendicular to its axis of rotation before it was suspended on ropes through a rotational wheel mounted at each side of the box. The box was then rotated (like a tombola) for one minute in one direction and another minute in the opposite direction. With a controlled stop the free surface was left sufficiently horizontal to form a rectangular material volume.

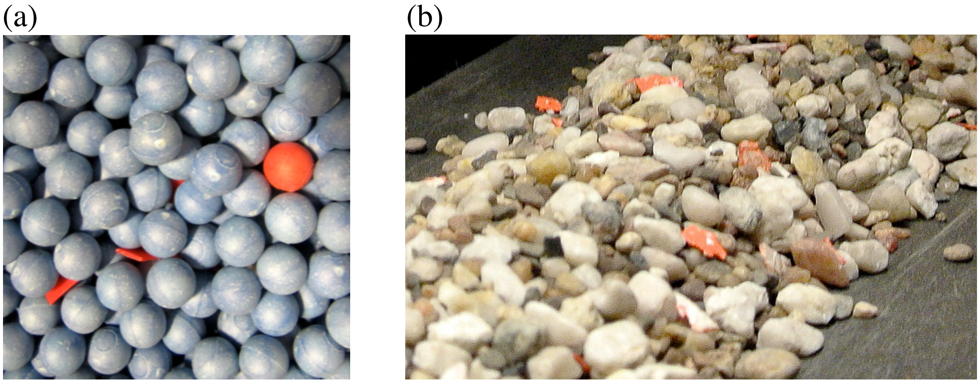

Figure 2: Material batches. (a) PVC balls and square polypropylene plates.
(b) Natural 2-8 mm river gravel with 2-8 mm shredded polypropylene flakes.

3.2 Sized distributed batch

3.2.1 Natural gravel and plastic flakes

The materials in the 30kg batch are shown in Fig. 2b. The batch had a size range 2-8 mm and was composed of sieved Dutch river bed gravel and shredded polypropylene flakes to simulate a concrete demolition waste stream with polluting plastics. Table 2 shows the detailed composition and particle properties. It is remarked that absolute accuracy in numbers is practically unobtainable because the gravel is abrasive during handling. Therefore a maximum of six tests was performed during which the batch composition could still be considered constant. This applied to three dry batches and three moist batches (0.5 to 0.9 litre water added per batch) to investigate the influence of possible particle segregation mechanisms.

Table 2: Composition of the 2-8 mm gravel batch when deposited onto the belt. γ is the ratio of batch bulk density and gravel mass density. For the calibration of packing and bulk density a larger gravel volume was used with the bulk density 1624 kg/m^3 and γ= 0.605.

	particles		**batch**		
	mass	density	Nr particles	mass	bulk density
Gravel 2-4 mm	0,0403 g	2685	383586	15.459 kg	1586 (γ= 0.591)
Gravel 4-8 mm	0.368 g		39100	14.401 kg	
Plastics 2-4 mm	0.00706 g	910	2294	16.2 g	
Plastics 4-8 mm	0.0290 g		1468	42.6 g	

3.2.2 Conveyor belt setup

Figure 3 shows the setup for controlled feeding of the granular batch to a conveyor belt (0.35 m/s). The pre-mixed material is poured into a plastic funnel (diameter top 200 mm, bottom 35 mm). Gravity then deposits the material onto a shortened shaker, which serves only to increase the material flow from the funnel. The material then flows with minimal height difference and disturbance onto the moving belt. The feeding is tuned so the material bed height on the belt is on average 14.5 mm and has a width of at least 45 mm for moist material (350 g/s feeding) and 75 mm for dry material (450 g/s feeding). Note therefore that the moist material is more viscous and flows slower. A belt-synchronized counter-rotating roller (cf. insert Fig. 3) slightly compresses the top of the material to create a flat bed of at least 35 mm wide and 14 mm high. It is noted the roller should not crush the material since that would disturb the homogeneity of the material bed. Behind the roller a laser triangulation sensor measured accurately the average height of the bed, which proved to be only 13 mm as the material slightly sags while being moved by the belt. Directly following the laser is a video camera that recorded the free surface in real-time (not shown in Fig. 3). The video stream is analysed for the time that the belt feeding is stationary to count the number of red plastics appearing within the 35 mm wide strip of the material bed.

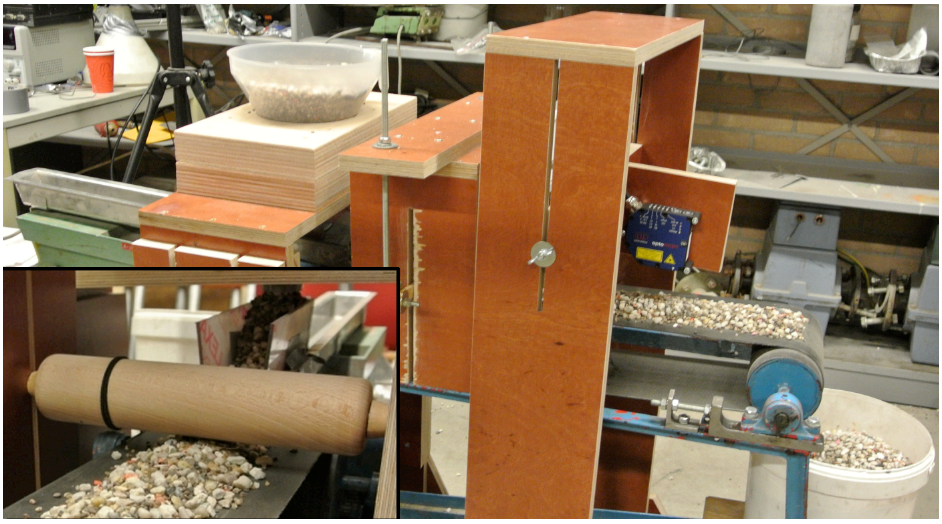

Figure 3: Conveyor setup for testing the gravel batches. The front-view inset (bottom left) shows the feed onto the belt and the roller that flattens the top of the material bed.

4. RESULTS AND DISCUSSION

4.1 Uniform batch

To validate the theory, which is based on uniform sized particles, we experimented with an oiled and a dry ball batch. Each was subjected to a series of thirty mixing experiments to study the convergence of the statistics. The packing shown in Fig. 1a matches the material for a compaction parameter C_A=1.06. Table 1 list the parameters. The number of spheres resulting from the model packing was 5940 against 5800 balls in the experiment. The experimental ratio of balls to plates was restored in the model by increasing the plates from 58 to 59.4 in accordance with Eq. (6). Here we first define the standard deviation for a binomial distribution

STD^B and the standard STD^S (68% probability):

$$STD^{B}=\frac{1}{30}\sum_{k=1}^{30}\sqrt{x_k}\,,\qquad STD^{S}=\frac{1}{\sqrt{29}}\sum_{k=1}^{30}\left|x_k-\bar{x}\right| \qquad \text{Eq. (8)}$$

Here x_k is the number of observed surface plates in an experiment and $\bar{x}$ is the average of the series. The mean value and STD of the number of observed surface plates after each experiment are shown in Fig. 4, where a red line indicates the predicted homogenous level. The expected number of red control balls over 30 tests is 9 with an STD^B of 3. Table 3 shows the control in both tests is within 1 STD^B, indicating the mixing was effective. The mean values are a bit higher than the homogenous level in Eq. (7) by 1.69 (oiled) and 1.59 plates (dry). The main cause was that the free surface was rather disorganized with a height variation of one ball diameter. This roughness effectively increased the surface and thus the expected number of plates counted. In fact, it can be shown that 23% of the plates embedded in the second layer were erroneously counted as being part of the upper layer. The influence of this surface condition will be relatively smaller for a larger surface and for increasing plate contents (but within the validity of the approximation $1-p \approx 1$ in Eq. (1)). The experimental STD converges to a value slightly below the homogenous level, suggesting lower uncertainty. To investigate, Tab. 3 shows all the converged values and STD.

Table 3: Comparison of converged experimental results and homogeneous level from the theory.

Plates	**Experiments**				**Homogenous level**	
	mean	STD^B	STD^S	control	mean	STD^B
Oiled	8.87	2.98	2.60	9	7.18	2.68
Dry	8.77	2.96	2.28	12	7.18	2.68

The experimental STD^S are 13% (oiled) and 23% (dry) lower than the experimental binomial STD^B. This difference indicates that on average the experiment is not fully described by a binomial distribution. The consistent lower uncertainty points to experimenter bias as a consequence of the disorganized material surface that demanded a consistent experimental approach to the interpretation of the visible plates. This unwittingly may have had a small stabilizing effect.

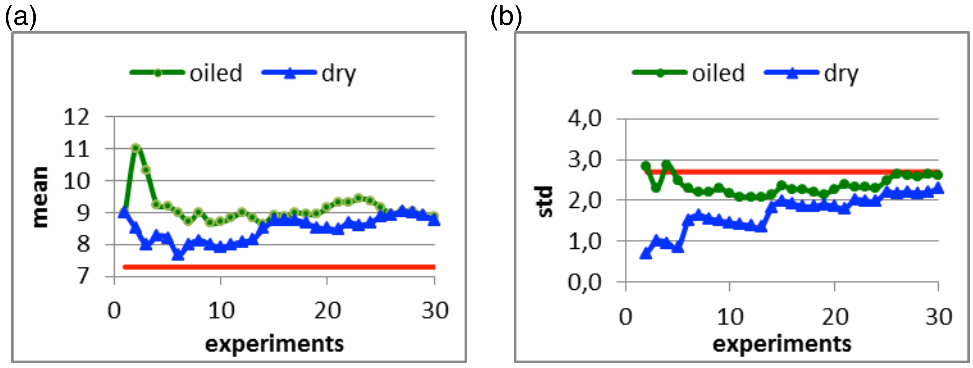

Figure 4: Experiments and homogenous level for square plates with an edge length equal to the ball diameter. (a) Mean plate count. (b) Standard deviation (68% probability).

Judging from Fig. 4, it may first be concluded that the applied mixing procedure was too short to reach full mixing and should preferably have been extended to the duration of 5 runs (200 box rotations) for oiled materials and at least another 15 runs (600 box rotations) for dry materials. Since the oil mainly suppresses plate percolation, this must be the prime cause of the slower convergence for the dry material. However, as the second conclusion, the fact that both materials do converge shows that our mixing procedure on the long run is effective and overcomes the segregation mechanisms inherent to the setup.

4.2 Size-distributed batch

We extend the theory by applying it to a 2-8 mm batch of gravel and plastic flakes. To this end we first introduce the sphere as the uniform particle to represent the average gravel shape and size. Experimental characterization of a large sample of gravel in the two size ranges showed the average grain is close to an ellipsoid with sieve-size normalized elliptical axes 0.7:1.0:1.41 (2-4 mm) and 0.64:1.0:1.51 (4-8 mm), where the middle size is identified as the sieve size. However, noting that the product of the axes is nearly unity, the volume of each ellipsoid is equal to that of a sphere with the same sieve size, validating the choice for a sphere. Next we introduce a square plate to represent all flake shapes as produced by a shredder. The average size of the plate is determined as follows. First we calculate for each size fraction the average edge length for a square plate of 1 mm thick from the number of flakes and their total mass. Next, the effective edge length is calculated from the average number-weighted sum for the two size fractions. The results are an average sphere diameter of 3.29 mm and average plate size of 3.90x3.90x1 mm. These two sizes are close enough to use the cubic positioning cell shown in Fig. 1c. For a compaction parameter C_B=1.01 the packing shown in Fig. 1b matches the bulk density of the gravel in a large calibration volume and therefore also in the experimental volume on the conveyor belt. The number of uniform spheres resulting from the model packing was 3.13e5 against 4.23e5 granules in the size range 2-8 mm in the experiment. The experimental ratio of granules to flakes was restored in the model by lowering the number of flakes from 3762 to 2783 in accordance with Eq. (6). Using Eq. (2)-(5) and (7), the calculated expected number of plastic flakes is 947. Note that this number also holds for the moist batches where the moisture acts merely as a sticking agent. To compare results from the different tests we normalize them to 100 s of stationary feeding. The results are shown in Tab. 4.

Table 4: Comparison of detected flakes in a 100 s video of a 35 mm wide strip of material (13 mm high) on the belt for three moist and three dry gravel batches. The right column shows the mean and STD^S (68% probability) of the three tests w.r.t. to the theoretical homogenous level.

Batch	Nr flakes	theory	deviation %	mean / STD^S
Dry	860	mean = 947 STD^B = 31	-9.2	-4.3 / 5.6
Dry	964		1.8	
Dry	895		-5.4	
Moist	869		-8.2	2.1 / 9.4
Moist	1046		10.4	
Moist	986		4.1	

The moisture had a clear influence on the results due to the smaller particles that have a larger surface to volume ratio. Even so, the average deviation from the predicted homogeneous level is only 4.3% lower for the dry materials and 2.1% higher for the moist ones. Although percolation is the obvious culprit for the lower number in the dry case, the moist materials introduced their own segregation effect. When moist material is poured into the plastic funnel the flat flakes may get temporarily stuck to the wall before they are flushed downwards by the material flow. This time delay tends to agglomerate moist plastic flakes at the funnel surface. Due to the way of feeding the belt, this translates to a higher concentration of flakes at the surface of the material bed on the belt. This effect is subtle and went undetected during our tests. However, it became clear when we deliberately increased the moisture content and some flakes were still sticking to the funnel wall after the test. A countermeasure would be to align the funnel with the same plastic mesh as described in Section 3.1. In a practical environment it can be difficult to maintain a low moisture content (<5 wt%) since granular materials dry quickly. However, judging from the higher STD^S in Tab. 4 for moist materials it appears that controlling the moisture content of the materials is vital for a stabile plate count.

5. CONCLUSIONS

This work introduces a theory to predict the homogenous statistics of a mix of granules with a minority of flat plates. The theory offers a simple way to assess homogeneity of this type of material by merely counting the number of plates that are visible in or on the upper layer of the free top surface. The theory is first put to the test using a uniform material composed of balls and plates. These tests validate the theory when taking account of the influences of surface roughness, which is inherent to natural granular materials. Subsequently the theory was extended to a 2-8 mm granular stream of gravel and plastic flakes to simulate a concrete waste stream on the lab-scale. The employed dry and moist gravel batches produced statistics that deviated by only a few percent from the predicted homogenous level. Combined with the sign of the deviation this was sufficient to identify and localize two particle segregation mechanisms in the setup as the most probably causes. In follow-up research we will build on the proposed theory to cover more complicated granular mixes including the influence of a disorganised surface. The aim will be to develop a reliable quantitative description for the more complex shaped particles encountered in waste streams such as recycled concrete aggregates [Tam, 2009].

AKNOWLEDGEMENTS

This work was financially supported by the European Commission in the H2020 collaborative project HISER, Grant Agreement No. 642085.

REFERENCES

Bonifazi G., Palmieri R. and Serranti, S. (2015). Hyperspectral imaging applied to end-of-life (EOL) concrete recycling. Technisches Messen, vol 82, nr 12, 616-624

Xia H. and Bakker M.C.M. (2014). Reliable classification of moving waste materials with LIBS in concrete recycling. Talanta, vol. 120, 239–247

López-Gayarre, F., Serna, P., Domingo-Cabo, A., Serrano-López, M.A. and López-Colina, C. (2009). Influence of recycled aggregate quality and proportioning criteria on recycled concrete properties. Waste Management, vol. 29, nr. 12, 3022-3028

Xia H. and Bakker M.C.M. (2013). Online Sensor System Based on Laser-induced Breakdown Spectroscopy in Quality Inspection of Demolition Concrete, Procedings ICSW, 27th International Conference on Solid Waste Technology and Management, Philadelphia.

Ottino J.M. and Khakhar D.V., 2000. Mixing and segregation of granular materials. Annu. Rev. Fluid Mech. vol 32, 55–91

Schröter, M., Ulrich, S., Kreft, J., Swift, J.B. and Swinney, H.L. (2006). Mechanisms in the size segregation of a binary granular mixture. Phys. Rev. E , vol 74, nr 1, 011307

Oversteegen, S.M. and Lekkerkerker, H.N.W. (2004). Phase diagram of mixtures of hard colloidal spheres and discs: A free-volume scaled-particle approach. J. Chem. Phys., vol. 120, nr. 5, 2470-2474

Tam, V.W.Y. and Tam, C.M. (2009). Parameters for assessing recycled aggregate and their correlation. Waste Management and Research, vol. 27, nr 1, 52-58